doi: 10.31674/book.2024ecc.005

Oxidation of Nitrite by an $\{Mn_4O_6\}^{4+}$ Core in Aqueous Media: Proton Coupled Electron Transfer

Suranjana Chatterjee

Department of Chemistry, Ananda Mohan College, Kolkata, West Bengal, India

Corresponding Author's Email: ranjanasur@yahoo.com

Abstract

Nitrous acid and its conjugate base nitrite are quantitatively oxidised to N(V) species in aqueous acidic (pH 2.0-6.0) media by a tetranuclear higher valent manganese complex $[Mn_4(\mu\text{-}O)_6(bipy)_6]^{4+}$(1, bipy = 2,2′-bipyridine), and its conjugate acid $[Mn_4(\mu\text{-}O)_5(\mu\text{-}OH)(bipy)_6]^{5+}$ ($1H^+$). As usual, protonated metal oxidant $1H^+$ reacts faster than 1, but an unusual observation of these reactions is the kinetic predominancy of HNO_2 over its conjugate base NO_2^-. Title complex 1 is stable in aqueous media over a long pH region and shows no ligand dissociative equilibria in the presence or absence of reducing agent. The reaction shows a remarkable kinetic isotope effect by increasing the reaction rate in D_2O media. A hydrogen atom transfer (HAT) mechanism (1e, $1H^+$; electroprotic) is appropriate to explain the isotope effect.

Keywords: *Isotope Effect; Kinetics; Manganese; Nitrite*

Introduction

Molecular dioxygen is generated in living systems by photosynthesis with the help of the oxygen evolving complex (OEC), which contains four manganese atoms at the reaction centre in close proximity to one another (Kirby *et al*., 1981; McEvoy & Brudvig, 2004; Yamaguchi *et al*., 2022; Burnap *et al*., 2022). The Mn aggregate is capable of cycling between five distinct oxidation levels, labeled as S_0 – S_4, as was demonstrated in the pioneering work of Kok, Forbush and McGloin (1970), which involves metal oxidation states II–IV (Dekker *et al*., 1984).

The site would contain two di-μ-oxo units linked by a μ-oxo-bis-μ-carboxylate bridge. The chosen oxidant $[Mn_4(\mu\text{-}O)_6(bipy)_6]^{4+}$ (**1**, Figure 1, bipy = 2,2′-bipyridine) of this study is topologically equivalent to Klein's proposal for OEC. Its one-electron reduced species, mixed-valent $Mn^{IV}_3Mn^{III}$ form, resembles the EPR spectroscopic model for the S_2 state (Philouze *et al*., 1994).

The N(III) atoms in the form of HNO_2 or NO_2^- have a varied redox role (Wilmarth *et al*., 1983; Rhodes, Barley & Meyer, 1991; Wu *et al*., 2020) in both oxidation and reduction purposes. The overall reactivity of N(III) in aqueous media not only results from NO_2^- and HNO_2, but also depends on the acidity of the aqueous solution and the total concentration of reagents used. NO^+ or even different redox species like NO, NO_2 and

N_2O_3 with notable acid-base features have a significant contribution to the reactivity. The study of aqueous N(III) chemistry thus remains a fertile endeavor. In view of the above discussion, it is believed that the redox reactivity of the title oxidant with N(III) will be informative in understanding the electron transfer mechanism in photosystem II.

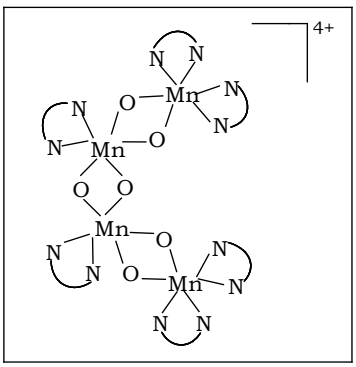

Figure 1: Schematic drawing of $[Mn_4(\mu\text{-}O)_6(bipy)_6]^{4+}$. $\overset{\frown}{N\quad N}$ is 2,2′-bipyridine
(Source: Das & Mukhopadhyay, 2007b)

Experimental

Materials

Pure crystals of title salt hydrate $[Mn_4(\mu\text{-}O)_6(bipy)_6](ClO_4)_4.2H_2O$ (**1**) were prepared according to the method described (Philouze *et al*., 1994). The tetrameric compound 1 used in all the experiments, thus seems to be almost pure monohydrated species. The solution of complex in water is stable in acidic environment up to pH 6.0. Sodium nitrite solution was prepared by dissolving recrystallised $NaNO_2$ in a hot ethanol-water mixture. The stock nitrite solution was standardised against $KMnO_4$. All used solutions were found to be unchanged for at least 24 hours at 10 °C and in a lower pH range up to pH 6.0.

$NaNO_3$ solution was standardised with a Dowex cation-exchange resin (in acid form), and the effluent acid was titrated with a standard base solution of NaOH with phenolphthalein indicator. 2,2′-bipyridine (G. R., E. Merck) solid was used as received without any further purification. D_2O (99.9 atom % D, Sigma) was used for the measurements of kinetic isotope effects. DNO_3 (99+ atom % D) was also from Sigma. Sulfanilic acid and a-naphthylamine were of E. Merck, G. R. grade. All other chemicals were of reagent grade. Throughout the experiments, doubly distilled deionized water was used to prepare all the solutions.

Equilibrium measurements

pH-metric titrations were performed to evaluate dissociation constants (K_a) of the acid HNO_2 in 95% D_2O media using a Metrohm 736-GP-Titrino autotitrator at I = 1.0 M ($NaNO_3$) at 25 °C. Similar methods were tried for the title complex over a long pH scale 2.0 – 8.0 to check oxo-bridge basicity.

Stoichiometric measurements

Overall stoichiometry of both reactions was determined in both kinetic ([reagent] >> [complex]) and non-kinetic conditions ([complex] > [reagent]). Unused amount of N(III) in the final solution state were colourimetrically determined, when 0.5 – 1.50 mM of 1 was allowed to react with 2.5 – 7.5 mM of reducing agent. After appropriate dilution, the remaining reaction mixtures were tested with sulfanilic acid and a-naphthylamine when a characteristic red dye was measured at 520 nm ($\varepsilon = 4.0 \times 10^4\ M^{-1}\ cm^{-1}$). The only reaction product, nitrate (NO_3^-) was detected by following the same procedure described above, but only Zn dust was added before the coupling reaction. Quantitative generation of NO_3^- was detected by the above method from the solutions having complex N(III) ratios between 1 : 2 to 1 : 4. The Mn complex, Mn^{II}, bipy and ClO_4^- did not interfere in this colorimetric study. Quantitative generation of bivalent manganese as the ultimate end product of the reduction could be estimated by complexometric method. In kinetic condition, an aliquot of the final product solutions was adjusted at pH 10 by ammonia-ammonium chloride buffer and estimated with standard EDTA using EBT indicator. At the end point, colour of the solution sharply changed from red to blue. It was also verified that other chemical species present in the product solution did not interfere in the complexometric titration. In non-kinetic situation, the tetrameric complex (0.10 – 0.50 mM) solution was allowed to react with the reagent concentration, which was less than the stoichiometric amount. After a definite interval of time, the absorbance of equilibrated solutions was measured at 420 nm ($\varepsilon = 7.5 \times 10^3\ M^{-1}\ cm^{-1}$) to evaluate the amount of Mn_4 complex left unreacted.

Physical measurements and kinetics

All physical parameters, like absorbances and spectra, of the described reaction were recorded with a Shimadzu (1601 PC) spectrophotometer using 1.00 cm quartz cells. The kinetics was monitored *in situ* with the instrument in “kinetic mode” at 420 nm in an electrically controlled thermostated 25.0(± 0.1) °C cell housing (CPS –240 A).

Except the Mn oxidant all other reaction partners are transparent at that (420 nm) wavelength. The ionic strength was normally maintained at 1.0 M with $NaNO_3$. Ligand bipyridine used in excess concentration (1 – 80 mM) over the complex, (C_{bipy} = [$(Hbipy)^+$] + [bipy]) acted as a good buffer. The pH value is increased by 0.4 units in D_2O media relative to the measured pH in water medium. In all the kinetic measurements, reducing agents were maintained in excess of the complex concentration.

Results and Discussion

Equilibrium measurements

The pK_a values of the title acid N(III) in 95% deuterated media and in aqueous media are found to be 3.80 ± 0.10 (Das & Mukhopadhyay, 2005) and 3.00, respectively. at 25.0

^{o}C and at I = 1.0 M ($NaNO_3$). Several attempts have been made to evaluate any ionisation constant for the oxidant in the working pH region (2.0–6.0) but have not resulted in any value.

Stoichiometric measurements

Stoichiometric determinations result in the average value $\triangle[Mn^{IV}_4]/\triangle[T_R]= 0.25 \pm 0.02$ where T_R = [N(III)] = [HNO_2] + [NO_3^-] i.e., analytical concentration of the reducing species. EDTA titration revealed that Mn^{II} is the final state of complex 1 in almost quantitative way. The ultimate reduced form of the tetravalent-tetramer is divalent manganese, which exists as a Mn^{II}- bipy complex at working condition. Existence of this complex is confirmed by the superposition of the optical spectra of ultimate product solutions and the mixture of manganese nitrate and 2,2'-bipyridine under the same conditions. Equation (1) is able to describe all the above findings.

$$[Mn_4O_6(bipy)_6]^{4+} + 4NO_2^- + 4H^+ \longrightarrow 4Mn^{2+} + 4NO_3^- + 6bipy + 2H_2O \quad (1)$$

Kinetics

The findings of decay in absorbance vs. time of the above kinetics are graphically posted and it is fitted finely in a standard first-order decay curve for at least four half-lives. The coloured oxidant is the only photoactive species in the working wavelength region (380 – 500 nm) where it absorbs sufficiently and the reaction rate constants do not vary with the wavelength. Each k_0 value measured is the average of at least three independent determinations where the coefficients of variation (CV) were within a maximum of 3%. The decay in absorbances at 420 nm is recorded, and $\log_{10}$(absorbance) *versus* time plots are excellent straight lines ($r \geq 0.98$) and slope of these lines directly produces k_0, the first order rate constants. Observed rate constants increase parallelly with the acidity of the reaction condition. The rate of the reactions remained unchanged when the amount of externally added bipy was varied in the range of 3–80 mM. Constancy in the k_0 values with the variation of bipy concentration ruled out the chance of any ligand releasing equilibrium in the parent complex solution. The rate of the reactions exhibits first-order dependencies on total reductant agent concentration over the working pH region and no T_R independent term is collected in the overall reaction. The observed rate constants were also found to be identical when complex concentrations were varied (0.05 – 0.2 mM) or in the presence or absence of ambient light in the reaction media. The reaction rate increases with decrease in ionic strength in the higher pH region and the reaction rates remain unaltered with the variation of ionic strength in the lower pH range. All these effects of ionic strength variation demonstrate the reaction between oppositely charged species and between charged and neutral species, respectively, at different pH regions.

Table 1: *Some representatives first-order rate constants*

pH	T_R, M	C_{bipy}, mM	$10^4 k_0$, s^{-1}
2.50	0.05	3.0	491 (500)
2.82	0.05	3.0	197 (202)
3.14	0.05	3.0	74.0 (76.6)
3.78	0.05	3.0	11.2 (10.4)
4.18	0.05	3.0	3.44 (3.34)
4.75	0.05	3.0	0.74 (0.78)
5.15	0.05	3.0	0.28 (0.30)
5.56	0.05	3.0	0.11 (0.11)
4.69	0.025	3.0	0.43 (0.45)
4.69	0.075	3.0	1.39 (1.35)
4.67	0.01	3.0	1.81 (1.89)
4.15	0.05	20	3.66 (3.62)
4.13	0.05	50	3.81 (3.82)
4.13	0.05	80	4.03 (3.82)
3.22	0.05	20	57.8 (59.6)
3.24	0.05	50	58.9 (56.0)
3.23	0.05	80	59.2 (57.8)
4.71	0.05	3.0	1.06[a]
4.70	0.05	3.0	1.39[b]
2.51	0.05	3.0	496[a]
2.53	0.05	3.0	499[b]

[a]I = 0.5 M ($NaNO_3$). [b]I = 0.1 M ($NaNO_3$)

Source: Das & Mukhopadhyay,2007b

The oxidation of nitrite by the title complex (0.10 mM) at T = 25.0 ^oC, I = 1.0 M ($NaNO_3$). Values within the parenthesis are calculated from equation (9) using the rate constants reported in Table 2.

The observed pH variation of the aforesaid redox can be explained and justified by the following reaction scheme, where simultaneously two protic equilibria equation (2) and equation (3) are considered. Here RH represents the protonated reductant, HNO_2 and R^- stands for the corresponding deprotonated species, i.e., NO_2^-.

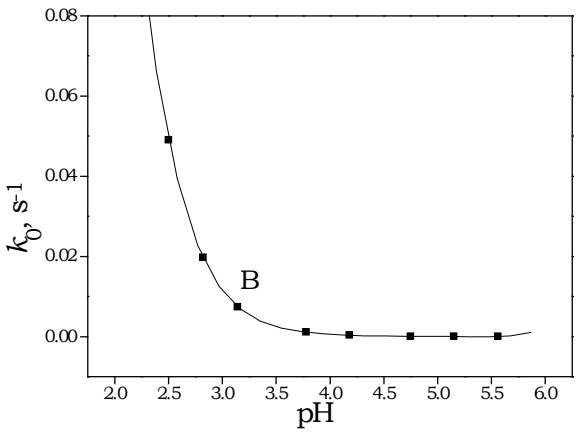

Figure 2: Plot of k_0 versus [H$^+$]. [complex]=0.10 mM, =25.0 °C, I=1.0 M ($NaNO_3$), C_{bipy}=3.0 *mM*
(Source: Das & Mukhopadhyay, 2007b)

$$RH \overset{K_a}{\rightleftharpoons} R^- + H^+ \quad (2)$$

$$\mathbf{1} + H^+ \overset{K_1}{\rightleftharpoons} \mathbf{1}H^+ \quad (3)$$

$$\mathbf{1}H^+ + RH \xrightarrow{k_1} \text{Products} \quad (4)$$

$$\mathbf{1}H^+ + R^- \xrightarrow{k_2} \text{Products} \quad (5)$$

$$\mathbf{1} + RH \xrightarrow{k_3} \text{Products} \quad (6)$$

$$\mathbf{1} + R^- \xrightarrow{k_4} \text{Products} \quad (7)$$

Scheme 1

The scheme 1 leads to the rate law equation (8).

$$k_0(1 + K_1[H^+])(K_a + [H^+])/T_R = k_1K_1[H^+]^2 + (k_2K_1K_a + k_3)[H^+] + k_4K_a \quad (8)$$

K_1 is the protonation constant of complex 1. The protonation occurs at the oxo-bridge of the oxidant. Several attempts have been made to evaluate the protonation constant of the title oxidant in the working pH range. Also, no pK_a value was obtained from the pH-meric titration of the complex soluton, indicating very weak basic nature of the oxo-bridges in water solution. Available literature reports on the study of numerous multicore higher-valent Mn complexes (Thorp *et al*., 1989) suggest the very weak basic nature of the oxo-bridges in an aqueous medium. Hence, from all the above information, it may be assumed that in this system, $K_1[H^+] << 1$. The maximum concentration of H$^+$ used is of the order of 10^{-2}. Therefore, $(K_1)_{max}10^{-2} << 1$, i.e., $(K_1)_{max} << 10^2$, so $(K_1)_{max} \leq 10$, i.e.,

the upper limit of K_1 is nearly at 10. Now, applying the assumption $K_1[H^+] << 1$, the equation (8) is simplified and takes the form described in equation (9).

$$k_0(K_a + [H^+])/T_R = k_1K_1[H^+]^2 + (k_2K_1K_a + k_3)[H^+] + k_4K_a \qquad (9)$$

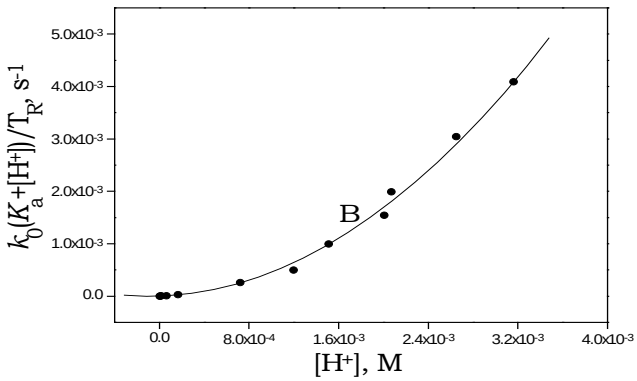

Figure 3: Plot of LHS of equation (9) versus $[H^+]$. [complex] = 0.10 mM, T = 25.0 °C, I = 1.0 M ($NaNO_3$), C_{bipy} = 3.0 mM *(Source: Das & Mukhopadhyay, 2007b)*

The left-hand side of equation (9) plotted against $[H^+]$, a well fitted polynomial curve obtain for the redox (Figure 3, $r > 0.98$), whence the rate parameters k_1K_1, ($k_2K_1K_a + k_3$) and k_4 (Table 2) were calculated. All these rate constants, if reused they reproduced experimentally observed k_0 values quite satisfactorily (within 7%). The k_0 values obtained from D_2O media also fit well with Scheme 1 and the rate parameters are determined in the same way, are listed in Table 2.

Table 2: *Rate constants for the reduction of 1 by nitrite at T = 25.0 °C, I = 1.0 M ($NaNO_3$)*

Reaction Path	k_1K_1 ($M^{-2}s^{-1}$)	($k_2K_1K_a + k_3$) ($M^{-1}s^{-1}$)	k_4 ($M^{-1}s^{-1}$)
H_2O medium	390 ± 20	$(8.2 \pm 0.5) \times 10^{-2}$	0
95% D_2O medium	760 ± 45	$(5.0 \pm 0.3) \times 10^{-2}$	0

(Source: Das & Mukhopadhyay, 2007b)

From Table 2, It can be noted that the value of k_4 path (**1**+R^- → Products) in both water and in D_2O media are statistically zero indicating non-existence of k_4 path. Eliminating k_4 term from equation (9), the polynomial changes to a simplified linear equation (10).

$$k_0(K_a + [H^+])/T_R = k_1K_1[H^+]^2 + (k_2K_1K_a + k_3)[H^+]$$

Dividing both side by $[H^+]$,

$$k_0(K_a + [H^+])/(T_R[H^+]) = k_1K_1[H^+] + (k_2K_1K_a + k_3) \qquad (10)$$

Thus, a plot of LHS of equation (10) *versus* $[H^+]$ (Figure 4) was found to be a straight line ($r > 0.98$) and slope $k_1K_1 = 384 \pm 15\ M^{-2}s^{-1}$ and intercept = $(8.0 \pm 0.3) \times 10^{-2}\ M^{-1}s^{-1}$.

The values of k_1K_1 and ($k_2K_1K_a + k_3$) obtained in the above-described manner are in close valuation (within 5%) with the reported values in Table 2, again confirming the absence of k_4 path in oxidation reaction.

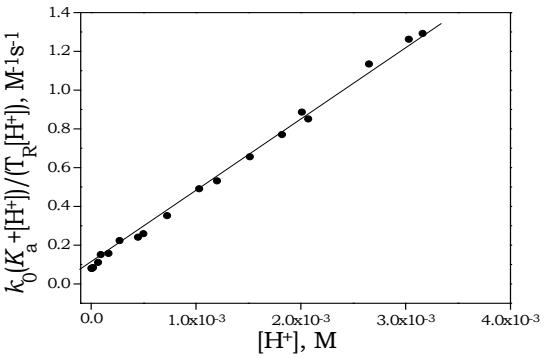

Figure 4: Plot of $k_0(K_a + [H^+])/(T_R[H^+])$ versus $[H^+]$. [Mn complex] = 0.10 mM, T = 25.0 °C, I = 1.0 M ($NaNO_3$) *(Source: Das & Mukhopadhyay, 2007b)*

An alternative to Scheme 1 that also explains the experimental findings is shown in Scheme 2 comprising only HNO_2 as reactive reductant.

$$\mathbf{1} + HNO_2 \xrightarrow{k'_2} \text{Products} \quad (11)$$

$$\mathbf{1}H^+ + HNO_2 \xrightarrow{k'_1} \text{Products} \quad (12)$$

Scheme 2

The calculated rate law for Scheme 2 is equation (13)

$$k_0/[HNO_2] = k'_1K_1[H^+] + k'_2 \quad (13)$$

Using the same procedure equation (13) is solved and obtain a good straight line with $k'_1K_1 = 390\ M^{-2}\ s^{-1}$ and $k'_2 = 0.082\ M^{-1}\ s^{-1}$. Value of the k'_1K_1 (reaction of $\mathbf{1}H^+$ with HNO_2) and k'_2 (reaction between **1** and HNO_2) path of Scheme 2 match well with the values reported for k_1K_1 and k_3 (taking k_2 path zero) in Scheme 1. Thus, this alternate scheme (Scheme 2) rules out any reactivity of nitrite anion with the tetrameric oxidant and with the protonated form of it. Therefore, the N(III) redox process is completely driven by the reactive protonated reductant HNO_2.

The alternative scheme (Scheme 2) of Scheme 1 for nitrite oxidation cannot confirm the non-reactivity of nitrite anion specially the non-existence of k_2 path i.e., the reaction between protonated metal oxidant ($\mathbf{1}H^+$) and the nitrite anion as the k_4 path which is the reaction between metal oxidant **1** and the NO_2^- is absent in scheme 1 also. Results of ionic strength variation at pH 4.7 (where $[NO_2^-] >> [HNO_2]$) indicated that reactions between oppositely charged ions as the first-order rate constants were decreased with

increasing ionic strength. Therefore, a significant role of the k_2 path may thus be expected when the k_4 path is totally absent in the kinetics. Protonated metal oxidants are kinetically superior to their deprotonated analogue, and hence **1**H^+ would oxidise NO_2^-. Kinetic differentiation of the k_2 and k_3 path is impossible due to proton-ambiguity of both the terms. It should be recalled that the k_1 path is effective towards the observed rate at pH $\leq$ 5.0. At lower pH, around pH 2.5 the kinetic superiority of acid form over its anionic conjugate form is reflected when media ionic strength is varied. The measured rate constants remain unaffected due to the change in ionic strength value of reactions indicating reaction between charged (**1** and **1**H^+) and neutral species (HNO_2).

From Table 2, It can be suggested that the maximum value of k_3 path (reaction between **1** and RH) would be 8.2×10^{-2} M^{-1} s^{-1} for N(III) oxidation.

Initially assumption was that $K_1[H^+]$ is much lower than **1**, and it draws an upper limit value for the K_1 of nearly 10. Taking the consideration that diffusion-controlled rate limit is 10^{11} M^{-1} s^{-1}, the assumed lower limit value of K_1 as found from the k_1K_1 value listed in Table 2 is around 10^{-9}.

Mechanism

The total eight electron transfers in this described redox are not in a single step but are the sum of several electronic transactions, but no immediate spectral changes were observed in working conditions. Moreover, in the working pH region, the linear dependence of k_0 on reagent concentration suggests a weak adduct formation, between the tetrameric Mn complex and the reducing agents. The electrochemistry of $[Mn_4(\mu\text{-}O)_6(bipy)_6]^{4+}$ has been extensively studied by Dunand-Sauthier *et al.* (1997, 1998, 1999). They prepared the title complex both electrochemically and chemically and also studied the electrochemical conversion of 1 into dinuclear ($[Mn^{III,IV}{}_2(\mu\text{-}O)_6(bipy)_4]^{3+}$) and mononuclear manganese ($[Mn^{II}(bipy)_3]^{2+}$) systems and *vice versa*. In nitric acid solution at pH = 2 the complex solution was decolourised upon application of 0.05 V *versus* SCE, indicates the final state is Mn^{II}. An overall eight electron reduction takes place. It is difficult to achieve the mono reduced form $[Mn^{IV}{}_3Mn^{III}(\mu\text{-}O)_6(bipy)_6]^{3+}$ by standard chemical reduction. The monoreduced form was generated by cryogenic radiolytic reduction of **1** (Blondin *et al.,* 1997) the very high reactivity of these monoreduced form was documented. This monoreduced one is not at all stable, even at low temperature (190 K). From the above discussion, it can be concluded that the tetrameric complex is not a powerful oxidant. The overall process of reducing the tetramer Mn^{IV} to Mn^{II} is a smooth transition, but initially, monoelectronic transfer to generate the mixed valent tetramer is energetically unfavourable process. In the overall reaction (equations 9 – 12), it is assumed initial mono electronic transfer is the rate limiting step, that produces the reactive intermediate $[Mn^{IV}{}_3Mn^{III}(m\text{-}O)_6(bipy)_6]^{3+}$, which is quickly reduced to final product form in the presence of excess reducing material or the produced radicals at the

rds. No polymerisation was observed when the reactions were carried out in a 6% v/v acrylonitrile solution, but this cannot prove the chance of the formation of radical as the radicals may react very fast with the mono-reduced Mn tetramer to initiate polymerisation. Basic nature of oxo-bridges of **1** or **1**H^+ tetramer highly increases due to one-electron reduction, which causes immediate grabbing of a proton from the reaction medium, which removes thermodynamic or kinetic barriers of reduction to the next level. The mono reduced form would have much more basic oxo-bridges, which could remove thermodynamic or kinetic barriers and facilitate further reduction (Baldwin & Pecoraro, 1996; Vrettos, Limburg & Brudvig, 2001) and it is one of the key points in the redox process of the Kok cycle in PS II (Renger, 2004).

In general, weak acids in H_2O become much weaker in D_2O, (Wiberg, 1955; Ghosh *et al*., 2002) and it was observed that pK_a's are considerably increased in D_2O for several reducing acids. Glyoxylic (Das, Bhattacharyya & Mukhopadhyay, 2006), pyruvic (Das, Bhattacharyya & Mukhopadhyay, 2006), nitrous (Das & Mukhopadhyay, 2007a) and hydroxylammonioum cations Therefore, for the tetrameric complex, the protonation constant (K_1) should increase in D_2O i.e., higher concentration of **1**H^+ is expected to be available in D_2O media compared to that in aqueous media. A structured network of hydrogen bonding in OEC is revealed during the molecular mechanics computation of the structure of the OEC cluster (Jeans *et al*., 2002; Russell & Vinyard, 2024; Matta, 2021), thereby providing an insight into the movement of proton and water in the site.

Conclusion

The reflection of the increase in K_1 value in D_2O media shows in the increment in k_1K_1 value, which effectively ruled over the decreased value of k_1 value (electroprotic mechanism). The reaction may be attributed to a secondary isotope effect where, during the substitution of isotopic (H *versus* D) no oxygen bonds to H/D are made or broken during the rate-limiting step and indicates that the isotopic atom is bonded more strongly through the H-bond in the transition state. This experimental fact again supports the existence of a postulated hydrogen-bonding network in the OEC. K_a value in D_2O media decreases compared to that in H_2O, which causes the lowering of the composite ($k_2K_1K_a$ + k_3) value in deuterated media. The contribution of the reaction path of NO_2^- with **1** in Scheme 1 towards the overall rate is found to be very small. Even, $(k_2K_1)_{max}$ value is found to be much lower than k_1K_1, therefore is expected a major contribution of k_3 path to evaluated composite term. Thus, in the described reduction process of tetramer (for both **1** and **1**H^+) the acidic format HNO_2 is more reactive than the conjugated basic form NO_2^-. The mechanistic pathways revealed the initial electron transaction by producing the nitrite radical ($NO_2^{\cdot}$) along with the protonated oxo-bridge in the mixed-valent tetramer in conjugation with a Hydrogen atom transfer (HAT) in the reducing agent. This mechanistic approach justifies the kinetic superiority of HNO_2 over its anion. In the protonated form of the tetramer **1**H+, a relatively stronger hydrogen bonding framework

forms between oxo-bridges and oxygens and hydrogens of the reducing species, which helps in the propagation of hydrogen or hydrogen ion and eventually this makes the species **1**H^+ kinetically superior.

Acknowledgment

The author thanks the higher authorities of Ananda Mohan College, Kolkata, India, for their continuous support.

References

Baldwin, M. J., & Pecoraro, V. L. (1996). Energetics of proton-coupled electron transfer in high-valent $Mn_2(\mu\text{-}O)_2$ systems: models for water oxidation by the oxygen-evolving complex of Photosystem II. *Journal of the American Chemical Society*, *118*(45), 11325-11326. https://doi.org/10.1021/ja9626906

Blondin, G., Davydov, R., Philouze, C., Charlot, M. F., Åkermark, B., Girerd, J. J., & Boussac, A. (1997). Electron paramagnetic resonance study of the S= ½ ground state of a radiolysis-generated manganese (III)–trimanganese (IV) form of $[Mn^{IV}_4 O_6 (bipy)_6]^{4+}$(bipy= 2, 2′-bipyridine). Comparison with the photosynthetic Oxygen Evolving Complex. *Journal of the Chemical Society, Dalton Transactions*, (21), 4069-4074. https://doi.org/10.1039/A703381H

Das, A., & Mukhopadhyay, S. (2005). Kinetic and Mechanistic Studies on the Oxidation of Nitrogen (III)(HNO_2/NO_2^-) by the Tris (biguanide) manganese (IV) Ion in Aqueous Acidic Media. *Helvetica Chimica Acta*, *88*(9), 2561-2572. https://doi.org/10.1002/hlca.200590195

Das, S., & Mukhopadhyay, S. (2007a). Mechanistic studies on oxidation of nitrite by a $\{Mn_3O_4\}^{4+}$ core in aqueous acidic media. *Dalton Transactions*, (22), 2321-2327. https://doi.org/10.1039/B702740K

Das, S., & Mukhopadhyay, S. (2007b). Oxidation of N^{III} and N^{-I} by an $\{Mn_4O_6\}^{4+}$ Core in Aqueous Media: Proton-Coupled Electron Transfer. https://doi.org/10.1002/ejic.200700363

Das, S., Bhattacharyya, J., & Mukhopadhyay, S. (2006). Mechanistic Studies on the Oxidation of Glyoxylic and Pyruvic Acid by a $[Mn_4O_6]^{4+}$ Core in Aqueous Media: Kinetics of Oxo-Bridge Protonation. *Helvetica Chimica Acta*, *89*(9), 1947-1958. https://doi.org/10.1002/hlca.200690186

Dekker, J. P., Van Gorkom, H. J., Wensink, J., & Ouwehand, L. (1984). Absorbance difference spectra of the successive redox states of the oxygen-evolving apparatus of photosynthesis. *Biochimica et Biophysica Acta (BBA)-Bioenergetics*, *767*(1), 1-9. https://doi.org/10.1016/0005-2728(84)90073-2

Dunand-Sauthier, M. N. C., Deronzier, A., & Piron, A. (1999). Electrochemical behaviour of $[Mn_2^{III,IV}O_2 (phen)_4]^{3+}$ complex in aqueous phen+ phenH+ buffer; phen= 1, 10-phenanthroline. *Journal of Electroanalytical Chemistry*, *463*(1), 119-122. https://doi.org/10.1016/S0022-0728(98)00429-X

Dunand-Sauthier, M. N. C., Deronzier, A., Piron, A., Pradon, X., & Ménage, S. (1998). New chemical and electrochemical synthesis of the $[Mn_4^{IV}O_6(bpy)_6]^{4+}$ Cluster. Electrochemical interconversion with corresponding Bi-and mononuclear complexes. *Journal of the American Chemical Society*, *120*(22), 5373-5380. https://doi.org/10.1021/ja974246o

Dunand-Sauthier, M. N. C., Deronzier, A., Pradon, X., Ménage, S., & Philouze, C. (1997). Electrochemical interconversion of mono-, bi-, and tetranuclear (bipyridyl) manganese

complexes in buffered aqueous solution. *Journal of the American Chemical Society*, *119*(13), 3173-3174. https://doi.org/10.1021/ja964102u

Ghosh, D., Shukla, A. D., Banerjee, R., & Das, A. (2002). Kinetics of oxidation of ascorbic acid and 1, 4-dihydroxybenzene by semiquinone radical bound to ruthenium (ii). *Journal of the Chemical Society, Dalton Transactions*, (6), 1220-1225. https://doi.org/10.1039/B104585G

Jeans, C., Schilstra, M. J., Ray, N., Husain, S., Minagawa, J., Nugent, J. H. A., & Klug, D. R. (2002). Replacement of tyrosine D with phenylalanine affects the normal proton transfer pathways for the reduction of $P680^+$ in oxygen-evolving photosystem II particles from Chlamydomonas. *Biochemistry*, *41*(52), 15754-15761. https://doi.org/10.1021/bi020558e

Kirby, J. A., Robertson, A. S., Smith, J. P., Thompson, A. C., Cooper, S. R., & Klein, M. P. (1981). State of manganese in the photosynthetic apparatus. 1. Extended x-ray absorption fine structure studies on chloroplasts and di-. mu.-oxo-bridged dimanganese model compounds. *Journal of the American Chemical Society*, *103*(18), 5529-5537. https://doi.org/10.1021/ja00408a042

Kok, B., Forbush, B., & McGloin, M. (1970). Cooperation of charges in photosynthetic O_2 evolution–I. A linear four step mechanism. *Photochemistry and Photobiology*, *11*(6), 457-475. https://doi.org/10.1111/j.1751-1097.1970.tb06017.x

Matta, D. K. (2021). *Role of Protonation State Changes and Hydrogen Bonding Around the Oxygen Evolving Complex of Photosystem II* (Doctoral dissertation, City University of New York).

McEvoy, J. P., & Brudvig, G. W. (2004). Structure-based mechanism of photosynthetic water oxidation. *Physical Chemistry Chemical Physics*, *6*(20), 4754-4763. https://doi.org/10.1039/B407500E

Oliver, N., Avramov, A. P., Nürnberg, D. J., Dau, H., & Burnap, R. L. (2022). From manganese oxidation to water oxidation: assembly and evolution of the water-splitting complex in photosystem II. *Photosynthesis Research*, *152*(2), 107-133. https://doi.org/10.1007/s11120-022-00912-z

Philouze, C., Blondin, G., Girerd, J. J., Guilhem, J., Pascard, C., & Lexa, D. (1994). Aqueous chemistry of high-valent manganese. Structure, magnetic, and redox properties of a new type of Mn-Oxo cluster,$[Mn_4^{IV}O4\ (bpy)_6]^{4+}$: relevance to the oxygen evolving center in plants. *Journal of the American Chemical Society*, *116*(19), 8557-8565. https://doi.org/10.1021/ja00098a016

Renger, G. (2004). Coupling of electron and proton transfer in oxidative water cleavage in photosynthesis. *Biochimica et Biophysica Acta (BBA)-Bioenergetics*, *1655*, 195-204. https://doi.org/10.1016/j.bbabio.2003.07.007

Rhodes, M. R., Barley, M. H., & Meyer, T. J. (1991). Electrocatalytic reduction of nitrite ion by edta complexes of iron (II) and ruthenium (II). *Inorganic Chemistry*, *30*(4), 629-635. https://doi.org/10.1021/ic00004a008

Russell, B. P., & Vinyard, D. J. (2024). Conformational changes in a Photosystem II hydrogen bond network stabilize the oxygen-evolving complex. *Biochimica et Biophysica Acta (BBA)-Bioenergetics*, *1865*(1), 149020. https://doi.org/10.1016/j.bbabio.2023.149020

Thorp, H. H., Sarneski, J. E., Brudvig, G. W., & Crabtree, R. H. (1989). Proton-coupled electron transfer in manganese complex $[(bpy)_2Mn(O)_2Mn(bpy)_2]^{3+}$. *Journal of the American Chemical Society*, *111*(26), 9249-9250. https://doi.org/10.1021/ja00208a029

Vrettos, J. S., Limburg, J., & Brudvig, G. W. (2001). Mechanism of photosynthetic water oxidation: combining biophysical studies of photosystem II with inorganic model chemistry. *Biochimica et*

Biophysica Acta (BBA)-Bioenergetics, *1503*(1-2), 229-245. https://doi.org/10.1016/S0005-2728(00)00214-0

Wiberg, K. B. (1955). The deuterium isotope effect. *Chemical Reviews*, *55*(4), 713-743. https://doi.org/10.1021/cr50004a004

Wilmarth, W. K., Stanbury, D. M., Byrd, J. E., Po, H. N., & Chua, C. P. (1983). Electron-transfer reactions involving simple free radicals. *Coordination Chemistry Reviews*, *51*(2), 155-179. https://doi.org/10.1016/0010-8545(83)85010-3

Wu, Y., Bu, L., Duan, X., Zhu, S., Kong, M., Zhu, N., & Zhou, S. (2020). Mini review on the roles of nitrate/nitrite in advanced oxidation processes: Radicals transformation and products formation. *Journal of Cleaner Production*, *273*, 123065. https://doi.org/10.1016/j.jclepro.2020.123065

Yamaguchi, K., Shoji, M., Isobe, H., Kawakami, T., Miyagawa, K., Suga, M., ... & Shen, J. R. (2022). Geometric, electronic and spin structures of the $CaMn_4O_5$ catalyst for water oxidation in oxygen-evolving photosystem II. Interplay between experiments and theoretical computations. *Coordination Chemistry Reviews*, *471*, 214742. https://doi.org/10.1016/j.ccr.2022.214742